Check for updates

View Article Online
View Journal

ChemComm
Chemical Communications

Accepted Manuscript

This article can be cited before page numbers have been issued, to do this please use: D. Sun, P. Li, X. Wang, Y. Wang, J. Wang, Y. Wang, Y. Lu, L. Duan, S. Sarina, H. Zhu and J. Liu, *Chem. Commun.*, 2020, DOI: 10.1039/D0CC03325A.

ROYAL SOCIETY OF CHEMISTRY

rsc.li/chemcomm

View Article Online
DOI: 10.1039/D0CC03325A

COMMUNICATION

Heterogeneous Photocatalytic Anaerobic Oxidation of Alcohols to Ketones by Pt-Mediated Hole Oxidation

Received 00th January 20xx,
Accepted 00th January 20xx

DOI: 10.1039/x0xx00000x

Danhui Sun,[a]† Peihe Li,[a]†* Xia Wang,[a] Yingying Wang,[a] Jinghui Wang,[a] Yin Wang,[a] Ye Lu,[a] Limei Duan,[a]* Sarina Sarina,[b] Huaiyong Zhu[b] and Jinghai Liu[a]*

We report a platinum nanocluster/graphitic carbon nitride (Pt/g-C_3N_4) composite solid catalyst with photocatalytic anaerobic oxidation function for highly active and selective transformation of alcohols to ketones. The desirable products were successfully obtained in good to excellent yield from various functionalized alcohols at room temperture, including the unactivated alcohols. Mechanism studies indicated that the reaction could proceed through a Pt-mediated hole oxidation initiating α-alcohol radical intermediate followed by a two-electron oxidation pathway. The merit of this strategy offers a general approach towards the green and sustainable organic synthetic chemistry.

Selective oxidation of alcohols to ketones is one of the most important reactions in organic synthetic chemistry, due to the ketones are widely used in production of fine chemical products such as perfumes, pharmaceuticals and organic intermediates.[1] Generally, ketones were obtained from alcohols in the presence of an additive oxidant under heating condition.[2] As a new developing trend for ketones synthesis, some studies have focused on the generation of ketones in the absence of additive oxidants, with hydrogen as the only by-product.[3] Converting alcohols into ketones by releasing hydrogen to support the anaerobic atmosphere and without using any additive sacrificial oxidants is a very interesting and important area needed to be further explored. Although research efforts have been made for the direct dehydrogenation of alcohols, it still need to be performed by reflux under high temperature, requiring extra energy input.[4] To date, the photochemisitry has provided a promising alternative for the oxidation of alcohols to ketones under mild conditions.[5] Various photocatalytic methods have been developed for the oxidation of alcohols to ketones under the aerobic[6] and anaerobic conditions.[7]

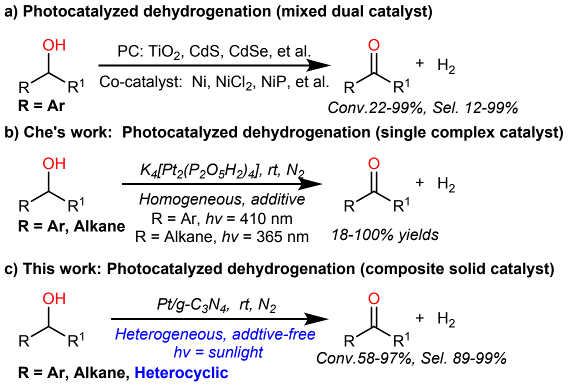

Scheme 1. Methods of photocatalytic dehydrogenation of alcohols under anaerobic conditions.

Recently, the photocatalytic dehydrogenation of alcohols without an additive oxidant has drawn extensive research attentions.[8] For instance, Xu and Xiao realized the oxidation of alcohols over an *in situ* Ni-modified CdS photocatalyst (**Scheme 1a**).[9] Wu and co-worker reported the dehydrogenation of alcohols under the help of 3-mercaptopropionic acid (MPA)-capped CdSe quantum dot and nickel(II) chloride,[10] et al (**Scheme 1a**). Most of these reactions used mixed dual catalysts, photocatalyst and metal-based co-catalyst, for the dehydrogenation of alcohols.[11] With considerations of the importance of sustainable and green requirements in synthetic chemistry, Che and co-workers employed a more attractive approach with a single complex catalyst, binuclear platinum(II) diphosphite complexes, for the oxidation of alcohols to ketones (**Scheme 1b**).[12] This protocol provides a simple and mild route for the dehydrogenation of alcohols under anaerobic conditions. Inspired by these progress and our continuing research interests in extending the application of graphitic carbon nitride photocatalysis,[13] to develop a new photocatalytic anaerobic oxidation for ketones synthesis.[14] Herein, we report a platinum nanocluster/graphitic carbon nitride (Pt/g-C_3N_4) composite solid catalyst with photocatalytic anaerobic oxidation activity for highly active and selective transformation of alcohols to

---

[a] *Inner Mongolia Key Laboratory of Carbon Nanomaterials, Nano Innovation Institute (NII), College of Chemistry and Materials Science, Inner Mongolia University for Nationalities Tongliao, 028000, China. E-mail: phli2018@foxmail.com, duanlmxie@126.com, jhliu2008@sinano.ac.cn.*
[b] *School of Chemistry, Physics and Mechanical Engineering, Queensland University of Technology, Brisbane, QLD 4001, Australia.*

† These authors contributed equally.

Electronic Supplementary Information (ESI) available: [details of any supplementary information available should be included here]. See DOI: 10.1039/x0xx00000x

View Article Online
DOI: 10.1039/D0CC03854A

Table 1. Optimization of the reaction conditions.[a,b]

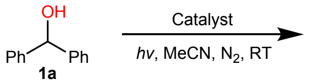

Entry	Catalyst	Conv. (%)	Sel. (%)
1	-	0	0
2	g-C_3N_4	5	99
3	Fe/g-C_3N_4	10	99
4	Cu/g-C_3N_4	8	99
5	Pd/g-C_3N_4	76	99
6	Ru/g-C_3N_4	96	99
7	Pt/g-C_3N_4	97	99
8[c]	Pt/g-C_3N_4	72	98
9[d]	Pt/g-C_3N_4	0	0
10[e]	Pt/g-C_3N_4	42	65
11[f]	Pt/g-C_3N_4	93	99
12[g]	Pt/g-C_3N_4	96	99
13[h]	Pt/g-C_3N_4	95	99
14[i]	Pt/g-C_3N_4	66	86

[a] Reaction conditions: **1a** (0.2 mmol), photocatalyst (5 mg) in MeCN (3 mL) under the irradiation of sun light at room temperature in N_2 atmosphere for 15 h. [b] Yields were determined by gas chromatography (GC) analysis using biphenyl as an internal standard. [c] Solvent: H_2O. [d] In darkness. [e] With 2,6-di*tert*-butyl-4-methylphenol (BHT) as a radical scavenger. [f] With benzoquinone as a superoxide scavenger. [g] With $AgNO_3$ as an electron scavenger. [h] With *tert*-butyl alcohol as a hydroxyl radical scavenger. [i] With ammonium oxalate as a hole scavenger.

ketones (**Scheme 1c**).

The microstructure of platinum nanocluster in Pt/g-C_3N_4 was examined by high-resolution transmission electron microscopy (HRTEM) and scanning transmission electron microscopy (STEM), where Pt nanoclusters with size about 2~3 nm are highly dispersed on the surface of g-C_3N_4 (**Figure S5**). The High-resolution Pt 4f XPS spectra reveals two valence states in Pt nanocluster for fresh Pt/g-C_3N_4 composite solid with Pt $4f_{5/2}$ at 77.6 eV (Pt $^{4+}$) and 75.6 eV (Pt $^{2+}$), Pt $4f_{7/2}$ at 74.3 eV (Pt $^{4+}$) and 72.3 eV (Pt $^{2+}$) (**Figure S6**). The photophysical property and bandgap structure of Pt/g-C_3N_4 were further characterized to show the thermodynamic potential for solar-driven photocatalysis (**Figure S2-S4**).

For the photocatalytic dehydrogenation of alcohols, we started our evaluation on the reaction parameters with benzhydrol (**1a**) as a model substrate. The oxygen-free photocatalytic dehydrogenation of benzhydrol was carried out under nitrogen atmosphere at room temperature. As shown in Table 1, no desired product diphenyl ketone (**2a**) was obtained in the absence of catalyst (**Table 1**, ***entry 1***). After the catalyst screening, we found that Pt/g-C_3N_4 and Ru/g-C_3N_4 afforded the desired product **2a** with the conversion of 97% and 96%, respectively, with both 99% selectivity (**Table 1**, ***entries 2-7***). Excitingly, replacing the solvent by pure water, Pt/g-C_3N_4 gave the conversion of **1a** in 72%, and the selectivity of product **2a** in 98%. The possible reason is that the substrate could not well dissolved in water, and water is also a competitor for the dehydrogenation during the reaction. In order to gain the mechanism insight into this photocatalytic selective oxidation reaction, we then conducted a series of control and trapping experiments. It is shown that no desired product was detected in the absence of light (**Table 1**, ***entry 9***). After adding a radical scavenger, 2,6-di*tert*-butyl-4-methylphenol (BHT), the conversion of **1a** dropped to 42% along with the selectivity of **2a** reducing to 65%, indicating that this reaction may proceed through a radical intermediate (**Table 1**, ***entry 10***). To further identify these radicals, the benzoquinone, $AgNO_3$ and *tert*-butyl alcohol were utilized as a scavenger for superoxide radical ($\bullet O_2^-$), electron and hydroxyl radical ($\bullet$OH) respectively, where we observed that the conversion of **1a** was not influenced (**Table 1**, ***entries 11-13***). Then, choosing the ammonium oxalate as a hole scavenger, both the conversion of **1a** and the selectivity of **2a** obviously decreased (**Table 1**, ***entry 14***), indicating a direct hole oxidation pathway in the reaction. It is interesting that the byproduct of 1,1,2,2-tetraphenylethane-1,2-diol (**3a**) was detected during the ammonium oxalate hole trapping experiment. For alternative hole trapping scavenger, $NaHCO_3$, the by-product of **3a** was also obtained. These results reveal that a α-alcohol radical intermediate may form in the reaction.

With the optimal reaction conditions in hand, we explored the scope of various alcohols. As shown in Table 2, all of the alcohols with the functionalized groups on the aromatic ring were oxidized smoothly to the corresponding ketones in moderate to excellent yield. The functional group on the side chains of aryl ring including H, Me, Et and Ph were examined under the optimal conditions. All of them were well tolerated and oxidized into the corresponding products in 67-97% conversions, and 95-99% selectivity (**Table 2**, ***2a-d***). We also tested the electron-withdrawing groups on the aryl ring including F, Cl, Br and CF_3, all of them can transform to the corresponding products in moderate to good conversion with excellent selectivity (**Table 2**, ***2e-h***). The electron-donating groups, e.g. Me and MeO, were well tolerated with 96-99% selectivities (**Table 2**, ***2i-l***). Then, the investigation on effects of *ortho-*, *meta-*, *para-* substitutions of aromatic rings shows that the conversion gradually decreased following the *para-*, *meta-*, *ortho-* sequence (**Table 2**, ***2j-l***). The reason may be the high steric resistance of substitution affecting the reaction kinetics. Furthermore, substrates of 1-naphthalenol and 9-fluorenol were also tolerated under the optimal conditions with good conversion and high selectivity (**Table 2**, ***2m-n***). We also examined the heterocycle (pyridine) in this reaction, the

Table 2. Photocatalytic reaction of aromatic alcohols.[a,b,c]

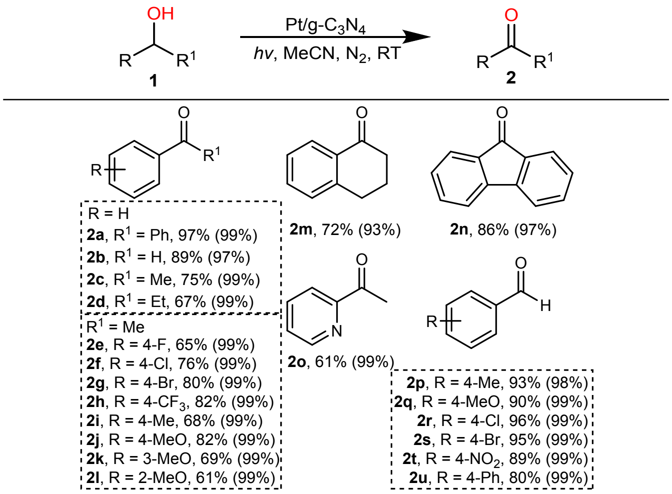

[a] Reaction conditions: **1** (0.2 mmol), Pt/g-C_3N_4 (5 mg) in MeCN (3 mL) under the irradiation of sun light at room temperature in N_2 atmosphere for 15 h. [b] Isolated yields. [c] Selectivity in parentheses.

View Article Online
DOI: 10.1039/D0CC03325A

Table 3. Photocatalytic reaction of aliphatic alcohols [a,b,c]

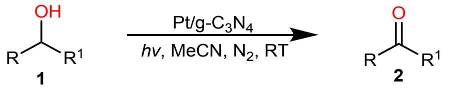

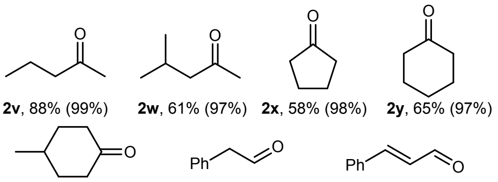

2v, 88% (99%) **2w**, 61% (97%) **2x**, 58% (98%) **2y**, 65% (97%)

2z, 80% (98%) **2aa**, 89% (99%) **2ab**, 58% (89%)

[a] Reaction conditions: **1** (0.2 mmol), Pt/g-C_3N_4 (5 mg) in MeCN (3 mL) under the irradiation of sun light at room temperature in N_2 atmosphere for 15 h. [b] Conversion were determined by GC analysis using biphenyl as an internal standard. [c] Selectivity in parentheses.

conversion of **2o** was 61%, and the selectivity was 99%. It is noting that the primary alcohol can also be transformed to the desired product in good conversion with high selectivity (**Table 2**, ***2b, 2p-u***).

Inspired by above exciting results, we next investigated the photocatalytic anaerobic dehydrogenation of aliphatic alcohols (**Table 3**). The anaerobic dehydrogenation of activated aliphatic alcohols is more challenging than benzylic alcohols due to the larger bond dissociation energies of aliphatic C–H bonds. It is exciting that under the optimal conditions, all of the aliphatic alcohols were well tolerated and transformed into the corresponding products in a moderate to good conversion with an excellent selectivity. The results indicate that the Pt/g-C_3N_4 makes the photocatalytic hole oxidation acting as a more effective approach towards the dehydrogenation of aliphatic alcohols under mild conditions.

To reveal the roles of Pt nanocluster in Pt/g-C_3N_4 for photocatalytic anaerobic dehydrogenation, hydrogen (H_2) production experiment was conducted using the benzhydrol without water as a model substrate (**Figure 1a**). No hydrogen was detected in the absence of photocatalyst, and with g-C_3N_4 as a control, a trace of hydrogen was detected. For Pt/g-C_3N_4, 225 μmol hydrogen was obtained, indicating that the Pt nanoclusters kinetically facilitated the photocatalytic dehydrogenation of H atoms from alcohol, and formation of H_2 molecules. Ruthenium (Ru) was also used as a control to examine the effects of nanocluster on the dehydrogenation and hydrogen production from alcohols, only 25 μmol hydrogen was obtained.

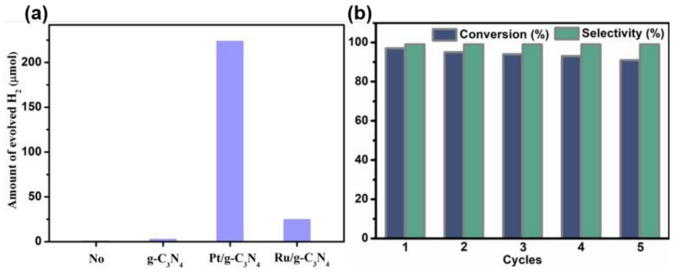

Figure 1. (a) Photocatalytic anaerobic dehydrogenation (Benzhydrol (5 mmol)). (b) Reusable features of heterogeneous Pt/g-C_3N_4 composite solid catalyst.

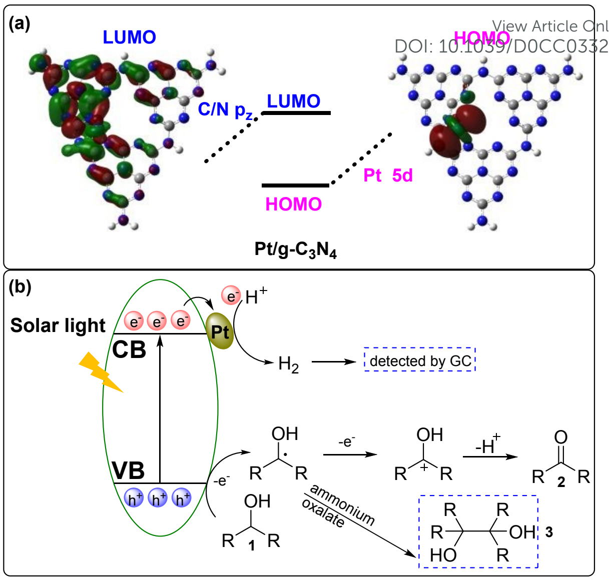

Figure 2. (a) DFT calculation for electronic structure of Pt/g-C_3N_4. (b) Proposed two-electron oxidation mechanism of photocatalytic anaerobic dehydrogenation of alcohols initiated by Pt/g-C_3N_4.

To further reveal the contribution of Pt-mediated hole oxidation during photocatalytic anaerobic oxidation, we have calculated the electronic structure of Pt/g-C_3N_4 by utilizing the Pt atom and heptazine unit for DFT calculations. The result shows that energy-favorable structure is the Pt atom coordinated with pyridinic-N in heptazine (Pt-N bond), where the highest occupied molecular orbital (HOMO) is mainly composed of 5d orbital (d_{z^2}) of Pt atom and lowest unoccupied molecular orbital (LUMO) consists of 2p orbital (p_z) of C and N atoms (**Figure 2a**). The Pt atom makes the LUMO and HOMO more localized (**Figure S10**), facilitating the separation and transfer of photogenerated hot electrons (holes) through the Pt-N tunnel, while the holes on the HOMO can oxidize the nitrogen atom to form the N^+-Pt states at the surface of solid catalyst which will initiate the dehydrogenation of alcohols. Based on the above results and related reports,[8-11] we proposed a possible two-electron oxidation mechanism for the photocatalytic anaerobic dehydrogenation of the alcohols (**Figure 2b**). Firstly, the holes (h^+) on the valence band (VB) and electrons (e^-) on conduction bond (CB) were generated under the irradiation of solar light.[6b,15] Then, the Pt mediated h^+ extracts hydrogen from the substrate **1** to release α-alcohol radicals.[6b,11a,15] Subsequently, the α-alcohol radical intermediate was oxidized to afford the corresponding product **2**.[11c] At the same time, the electrons in the CB band transferred to Pt nanoclusters through Schottky-junction to drive the formation of H_2 molecules.[11a] Furthermore, both the byproduct **3** and H_2 provided supportive evidences for the reaction mechanism of photocatalytic anaerobic dehydrogenation of alcohols.

The reusable features of Pt/g-C_3N_4 composite solid catalyst was evaluated by recycling the it to compare the conversion and selectivity of the model reaction (**Figure 1b**). The catalyst was available to reuse at least five times without significant loss of its catalytic activity. Interestingly, after the five cycles, the IR and XPS results show the stable microstructure of Pt/g-C_3N_4 after the photocatalytic anaerobic oxidation (**Figure S1** and

View Article Online
DOI: 10.1039/D0CC03325A

Figure S9), only with the binding energy of Pt changing into Pt $4f_{5/2}$ at 76.9 eV and Pt $4f_{7/2}$ at 73.5 eV. From the high-resolution Pt 4f XPS, we found that the two oxidation states with binding energy of Pt $4f_{5/2}$ at 77.6 eV and Pt $4f_{7/2}$ at 74.3 eV for Pt $^{4+}$ and Pt $4f_{5/2}$ at 75.6 eV and Pt $4f_{7/2}$ at 72.3 eV for Pt $^{2+}$ changed into one, indicating the valence state variation from two valence states into one. The high oxidation state of Pt $^{4+}$ in the composite solid (Pt/g-C_3N_4) experienced reduction as indicated by reducing the 0.8 eV binding energy for Pt $4f_{7/2}$, while low oxidation state of Pt $^{2+}$ appeared oxidation as shown by increasing 1.2 eV binding energy, indicating the occurrence of charge redistribution in the Pt/g-C_3N_4 during the photocatalytic process. From the DFT calculation (**Figure 2a**), we found the Pt-N coordinated bond acting as the electron transfer tunnel for the Pt nanocluster and g-C_3N_4 in the composite solid.

In summary, we have explored a new solar-driven hole oxidation approach enabled by a Pt/g-C_3N_4 composite solid catalyst for photocatalytic anaerobic dehydrogenation of alcohols to ketones with good conversion and high selectivity. Under oxygen-free mild conditions, the transformation sustainably proceeded and tolerated a broad range of functional substrates including unactivated alcohols. The reaction mechanism insights revealed a Pt-mediated hole oxidation initiating the α-alcohol radical intermediate and two-electron oxidation. This composite solid catalyst along with heterogeneous solar-driven hole anaerobic oxidation would open a sustainable approach towards the green and precise organic synthetic chemistry.

This work was financially supported by the National Natural Science Foundation of China (21961024, 21961025), Inner Mongolia Natural Science Foundation (2018JQ05, 2019BS02008, 2019BS02007). Supported by Incentive Funding from Nano Innovation Institute (NII) of Inner Mongolia University for Nationalities (IMUN). Inner Mongolia Autonomous Region Science & Technology Planning Project for Applied Technology Research and Development (2019GG261), and Inner Mongolia Autonomous Region Funding Project for Science & Technology Achievement Transformation (CGZH2018156). Inner Mongolia Autonomous Region Incentive Funding Guided Project for Science & Technology Innovation (2016). Scientific Research Projects of the Inner Mongolian Higher Educational System (NJZZ20110). IMUN Doctoral Research Startup Fund Project (BS445, BS437). IMUN Graduate Research Project (NMDSS1868, NMDSS1937).

Conflicts of interest

There are no conflicts to declare.

Notes and references

1 (*a*) Y. Qu and X. Duan, *Chem. Soc. Rev*., 2013, **42**, 2568–2580; (*b*) J. Wang, H. Liang, C. Zhang, B. Jin and Y. Men, *Appl. Catal. B,* 2019, **256**, 117874–117885.

2 T. Mallat and A. Baiker, *Chem. Rev.,* 2004, **104**, 3037–3058.

3 (*a*) I. E. Markó, P. R. Giles, M. Tsukazaki, S. M. Brown and C. J. Urch, *Science*, 1996, **274**, 2044–2046; (*b*) B. Guan, D. Xing, G. Cai, X. Wan, N. Yu, Z. Fang, L. Yang and Z. Shi, *J. Am. Chem. Soc*., 2005, **127**, 18004–18005.

4 (*a*) D. I. Enache, J. K. Edwards, P. Landon, B. Solsona-Espriu, A. F. Carley, A. A. Herzing, M. Watanabe, C. J. Kiely, D. W. Knight and G. J. Hutchings, *Science*, 2006, **311**, 362–365; (*b*) K. Fujita, T. Yoshida, Y. Imori and R. Yamaguchi, *Org. Lett*., 2011, **13**, 2278–2281; (*c*) R. Kawahara, K. Fujita and R. Yamaguchi, *J. Am. Chem. Soc*., 2012, **134**, 3643–3646; (*d*) R. Kawahara, K. Fujita and R. Yamaguchi, *Angew. Chem. Int. Ed.,* 2012, **124**, 12962–12966.

5 (*a*) N. Zhang, Y. Zhang, X. Pan, X. Fu, S. Liu and Y. Xu, *J. Phys. Chem. C,* 2011, **115**, 23501–23511; (*b*) B. Long, Z. Ding and X. Wang, *ChemSusChem*, 2013, **6**, 2074–2078; (*c*) O. Tomita, T. Otsubo, M. Higashi, B. Ohtani and R. Abe, *ACS Catal*., 2016, **6**, 1134–1144; (*d*) S. Meng, X. Ye, X. Ning, M. Xie, X. Fu and S. Chen, *Appl. Catal. B*, 2016, **182**, 356–368; (*e*) M. J. Lima, A. M. T. Silva, C. G. Silva and J. L. Faria, *J. Catal*., 2017, **353**, 44–53; (*f*) T. Zhu, X. Ye, Q. Zhang, Z. Hui, X. Wang and S. Chen, *J. Hazard. Mater*., 2019, **367**, 277–285.

6 (a) D. Tsukamoto, Y. Shiraishi, Y. Sugano, S. Ichikawa, S. Tanaka and T. Hirai, *J. Am. Chem. Soc*., 2012, **134**, 6309–6315; (b) W. Huang, B. C. Ma, H. Lu, R. Li, L. Wang, K. Landfester and K. A. I. Zhang, *ACS Catal*., 2017, **7**, 5438–5442; (*c*) Y. Chen, Z. U. Wang, H. Wang, J. Lu, S. Yu and H. Jiang, *J. Am. Chem. Soc*., 2017, **139**, 2035–2044.

7 (*a*) S. Higashimoto, Y. Tanaka, R. Ishikawa, S. Hasegawa, M. Azuma, H. Ohue and Y. Sakatab, *Catal. Sci. Technol*., 2013, **3**, 400–403; (*b*) Z. Liu, J. Caner, A. Kudo, H. Naka and S. Saito, *Chem. Eur. J.,* 2013, **19**, 9452–9456.

8 (*a*) G. Zhao, G. W. Busser, C. Froese, B. Hu, S. A. Bonke, A. Schnegg, Y. Ai, D. Wei, X. Wang, B. Peng and M. Muhler, *J. Phys. Chem. Lett*., 2019, **10**, 2075–2080; (*b*) H. Hao, L. Zhang, W. Wang, S. Qiao and X. Liu, *ACS Sustainable Chem. Eng*., 2019, **7**, 10501–10508; (*c*) Y. Hu, G. Zhao, Q. Pan, H. Wang, Z. Shen, B. Peng, G. W. Busser, X. Wang and M. Muhler, *ChemCatChem,* 2019, **11**, 5139–5144; (*d*) H. Fuse, H. Mitsunuma and M. Kanai, *J. Am. Chem. Soc.*, 2020, **142**, 4493–4499.

9 Z. Chai, T. Zeng, Q. Li, L. Lu, W. Xiao and D. Xu, *J. Am. Chem. Soc.,* 2016, **138**, 10128–10131.

10 L. Zhao, Q. Meng, X. Fan, C. Ye, X. Li, B. Chen, V. Ramamurthy, C. Tung and L. Wu, *Angew. Chem. Int. Edit.,* 2017, **56**, 3020–3024.

11 (*a*) F. Li, Y. Wang, J. Du, Y. Zhu, C. Xu and L. Sun, *Appl. Catal. B,* 2018, **225**, 258–263; (*b*) D. Jiang, X. Chen, Z. Zhang, L. Zhang, Y. Wang, Z. Sun, R. Irfan and P. Du, *J. Catal.,* 2018, **357**, 147–153; (*c*) X.-J. Yang, Y.-W. Zheng, L.-Q. Zheng, L.-Z. Wu, C.-H. Tung and B. Chen, *Green Chem*., 2019, **21**, 1401–1405; (*d*) H. Kasap, C. A. Caputo, B. C. M. Martindale, R. Godin, V. W. Lau, B. V. Lotsch, J. R. Durrant and E. Reisner, *J. Am. Chem. Soc.,* 2016, **138**, 9183–9192.

12 J. Zhong, W. To, Y. Liu, W. Lu and C. Che, *Chem. Sci.*, 2019, **10**, 4883–4889.

13 (*a*) J. H. Liu, T. K. Zhang, Z. C. Wang, G. Dawson and W. Chen, *J. Mater. Chem.,* 2011, **21**, 14398−14401; (*b*) J. H. Liu, Y. W. Zhang, L. L. Lu, G Wu and W. Chen, *Chem. Commun.,* 2012, **48**, 8826−8828; (*c*) J. Liu, S. Xie, Z. Geng, K. Huang, L. Fan, W. Zhou, L. Qiu, D. Gao, L. Ji, L. Duan, L. Lu, W. Li, S. Bai, Z. Liu, W. Chen, S. Feng and Y. Zhang, *Nano Lett.,* 2016, **16**, 6568−6575; (*d*) Z. Zhang, Y. J. Zhang, L. H. Lu, Y. J. Si, S. Zhang, Y. Chen, K. Dai, P. Duan, L. M. Duan and J. H. Liu, *Appl. Surf. Sci.,* 2017, **391**, 369−375.

14 (*a*) P.-H. Li, Z. Wang, H. Fu, Q.-P. Dai and C.-W. Hu, *Chem. Commun.,* 2018*,* **54***,* 12471–12474*;* (*b*) P. Li, Y. Wang, X. Wang, Y. Wang, Y. Liu, K. Huang, J. Hu, L. Duan, C. Hu and J. Liu, *J. Org. Chem.,* 2020, **85**, 3101–3105.

15 H. Ou, C. Tang, X. Chen, M. Zhou and X. Wang, *ACS Catal.,* 2019, **9**, 2949–2955.

View Article Online
DOI: 10.1039/D0CC03325A

COMMUNICATION